Article

Not peer-reviewed version

Impact of Amorphous-to-Crystalline Transition on the Upconversion Luminescence in Er3+-Doped Ga2O3 Thin Films

Yuanlin Liang , Haisheng Chen , Dianming Dong , Jiaxing Guo , Xiaona Du , Taiyu Bian , Fan Zhang , Zhenping Wu , Yang Zhang *

Posted Date: 5 February 2024

doi: 10.20944/preprints202402.0252.v1

Keywords: Amorphous-to-crystalline transition; Upconversion luminescence; Wide bandgap semiconductor; Thin films; Lanthanide doped phosphors

Article

Impact of Amorphous-to-Crystalline Transition on the Upconversion Luminescence in Er^{3+}-Doped Ga_2O_3 Thin Films

Yuanlin Liang [1], Haisheng Chen [1], Dianmeng Dong [2], Jiaxing Guo [1], Xiaona Du [3], Taiyu Bian [1], Fan Zhang [2], Zhenping Wu [2,*] and Yang Zhang [1,*]

[1] Institute of Modern Optics & Tianjin Key Laboratory of Micro-Scale Optical Information Science and Technology, Nankai University, Tianjin 300071, China
[2] State Key Laboratory of Information Photonics and Optical Communications & School of Science, Beijing University of Posts and Telecommunications, Beijing 100876, China
[3] Institute of Photoelectric Thin Film Devices and Technology, College of Electronic Information and Optical Engineering, Nankai University, Tianjin 300350, China
* Correspondence: yangzhang@nankai.edu.cn (Y. Zhang), zhenpingwu@bupt.edu.cn (Z. P. Wu)

Abstract: Gallium oxide (Ga_2O_3) is an emerging wide bandgap semiconductor promising a wide range of important applications. However, mass production of high-quality crystalline Ga_2O_3 still suffers from limitations associated with poor reproducibility and low efficiency. Low-temperature grown amorphous Ga_2O_3 demonstrates comparable performance with its crystalline counterparts. Lanthanide Er^{3+}-doped Ga_2O_3 (Ga_2O_3: Er) possesses great potential for developing light-emitting devices, photodetectors and optical waveguides. The host circumstance can exert a crystal field around the lanthanide dopants and strongly influence their photoluminescence properties. Here we present a systematical study of the impact of amorphous-to-crystalline transition on the upconversion photoluminescence in Ga_2O_3: Er thin films. Through controlling the growth temperature of Ga_2O_3: Er films, the upconversion luminescence of as-grown thin films are strongly enhanced over 100 times. Moreover, the variation of photoluminescence reflects the amorphous-to-crystalline transformation of the Ga_2O_3: Er thin films. These results will aid further design of favorable optoelectronic devices integrated with lanthanide-doped Ga_2O_3 thin films.

Keywords: amorphous-to-crystalline transition; upconversion luminescence; wide bandgap semiconductor; thin films; lanthanide doped phosphors

1. Introduction

Gallium oxide (Ga_2O_3) as an emerging wide bandgap semiconductor has sparked intense interest during the past years for its superior chemical and thermal stability, radiation hardness, and notably high breakdown electric field (~ 8 MV/cm) [1]. Owing to the unique electric and optical characteristics, Ga_2O_3 has been explored as the workhorse for applications such as solar-blind ultraviolet photodetectors, power electronic devices, etc [2–4]. Given the ultrawide bandgap, Ga_2O_3 is regarded as an ideal host material for incorporating lanthanide element [5]. Lanthanide ions, referred to as magic dopants, are highly effective in promoting the electrical properties of the host materials [6–8], moreover, lanthanide dopants can introduce an additional luminescent functionality to the semiconductor [9]. The most stable oxidation state of lanthanide elements is the trivalent state (Ln^{3+}), which exhibits efficient upconversion and downconversion luminescence. They demonstrate unique luminescent characteristics, including abundant energy levels, sharp emission bandwidths, large Stokes shift, and high photoresistance, making them an important class of phosphor materials [10–12].

Among lanthanide elements, Er^{3+}-doped phosphors exhibit strong visible and near-infrared emissions from its intra-4f shell transition of Er^{3+} ions, enabling diverse applications including full color displays, biological imaging, optical storage, optical communications [13–16]. So far, Er^{3+}-doped

 doi:10.20944/preprints202402.0252.v1

Ga_2O_3 has been developed for electroluminescence (EL) devices, light-emitting devices (LEDs), and photodetectors [17–20]. In terms of fundamental research and real applications, luminescent thin films are of great importance from both scientific and technological aspects [21]. To date, Er^{3+}-doped Ga_2O_3 thin films have been fabricated using pulsed laser deposition (PLD) and radio frequency magnetron sputtering methods on various substrates. Ga_2O_3 has five different polymorphs, including corundum (α), monoclinic (β), defective spinel (γ), cubic (δ), orthorhombic (ε) structures. Among them, β-Ga_2O_3 is the most stable form under ambient condition, and has been extensively investigated for various applications [22,23]. However, fabrication of single-crystalline β-Ga_2O_3 with a perfect stoichiometry remains a daunting challenge. Recently, low-temperature deposited amorphous Ga_2O_3 (a-Ga_2O_3) has demonstrated comparable optoelectronic properties with its crystalline counterparts [24]. Moreover, low-temperature fabricated a-Ga_2O_3 is compatible with mature CMOS technologies and favorable for flexible devices. It has been proven that a-Ga_2O_3 is qualified for high-performance X-ray and solar-blind photon detectors [25,26]. To date, there is no investigation on the luminescent properties of lanthanide-doped a-Ga_2O_3. The host circumstance can exert a crystal field around the lanthanide dopants and strongly influence their photoluminescence properties. According to the Judd-Ofelt theory, local symmetry around the doped lanthanide ions can render their radiative transition probabilities [27]. Previous studies have shown that growth temperature has a huge impact on the crystallinity of Ga_2O_3 [28]. Herein, we present an experimental investigation on the crystallinity of Ga_2O_3 host impact on the upconversion Photoluminescence (PL) from Ga_2O_3: Er thin films. The variation of photoluminescence clearly reflects the amorphous-to-crystalline transformation of the Ga_2O_3: Er thin films. We demonstrate a strong enhancement of the upconversion emissions associated with the improved crystallinity of Ga_2O_3 by increasing the growth temperature. These results identify the interplay between the crystallinity and the dopant lanthanide luminescence, which paves the way for developing lanthanide-doped Ga_2O_3 based optoelectronic devices.

2. Experiment

Target Synthesis: Er^{3+}-doped Ga_2O_3 targets were synthesized via high temperature solid-state reaction method using reagent grade Ga_2O_3 and Er_2O_3 powders as raw materials. Er^{3+}-doped Ga_2O_3 powders with different doping concentrations of 0.5 at%, 0.75 at%, 1 at%, 1.25 at% and 1.5 at% were prepared. The weighted Ga_2O_3 and Er_2O_3 powders were milled using alcohol for 3 h. And then, the obtained slurry was dried at 80 ºC. After that, the dried compounds were granulated with 10 wt% polyvinyl alcohol binder, pressed into disk-shaped pellets and sintered at 1450 ºC in air for 4 h.

Thin films Fabrication: Ga_2O_3: Er thin films were deposited on (0001) sapphire substrates by PLD using a 248-nm KrF excimer laser (Coherent COMPex205). Before deposition, sapphire substrates were ultrasonically cleaned in organic solvents, and rinsed in deionized water and blown dried with nitrogen gas. Then, the substrates were inserted into the growth chamber. A KrF excimer laser was used with a fluence of 1.5 J cm^{-2} and a repetition frequency of 5 Hz. The distance between target and substrate was set at 50 mm, the basic vacuum was below 1×10^{-4} Pa controlled by a turbo molecular pump. During the growth, the oxygen pressure was controlled to be 1 Pa. These films were achieved by setting different substrate temperatures including room temperature (RT), 300 ºC, 400 ºC, and 500 ºC. After the deposition of an hour, except for RT grown sample, other samples were slowly cooled down to room temperature.

Characterization and Luminescence Measurement: The X-ray diffraction (XRD) measurement was carried out with the Bruker D8 Advanced X-ray diffractometer under CuKα1 (λ = 1.5406 Å) radiation. The Scanning Electron Microscopy (SEM) was measured using a field emission scanning electron microscope (Zeiss Sigma 500). The UV/Vis absorption spectra were recorded with the Hitachi U-3900 UV/Vis spectro-photometer. The Photoluminescence spectrum was measured by an Acton SpectraPro 300i spectrophotometer. All upconversion spectra were excited by a 980 nm diode laser. The spectrum ranges from 480nm to 700nm. Transient decay curves were measured with a Tektronix DPO3034 oscilloscope combined with photomultiplier tube (H11902-04, Hamamatsu). All measurements were carried out at room temperature.

 doi:10.20944/preprints202402.0252.v1

3. Results and Discussion

The primary advantage of the PLD technology is the stoichiometric transfer of the target material to the grown film on the substrate. In order to filter out the most efficient luminescent composition, we prepared Er^{3+}-doped Ga_2O_3 powders with different doping concentrations from 0.5% to 1.5%. Figure 1a shows the XRD θ-2θ patterns of Er^{3+}-doped Ga_2O_3 powders with different doping concentrations. The characteristic diffraction peaks correspond to the monoclinic (β) phase of Ga_2O_3. The results imply that Er^{3+} ions are efficiently doped into Ga_2O_3 host. Besides the diffraction peaks of Ga_2O_3, small amount of secondary phase $Er_3Ga_5O_{12}$ (ErGG) appears along with the Ga_2O_3 phase. Note that the (420) peak at 32.6° of the secondary ErGG phase increases along with the concentration of Er^{3+} dopant. Compared with pure Ga_2O_3 shown in Figure 1a, there are minor left shifts of the diffraction peak (111) for the Er^{3+}-doped Ga_2O_3 samples as seen in the inset of Figure 1a. Considering that the ionic radius (0.881 Å) of the Er^{3+} ion is larger than that of Ga^{3+} ion (0.62 Å), it means that the lattice constant of Er^{3+}-doped Ga_2O_3 expands, contributing to the diffraction peaks shift to lower angles. Figure 1b shows the upconversion PL spectra of Ga_2O_3 powders doped with different Er^{3+} ion concentrations. The typical upconversion spectra of Er^{3+} consist of strong green and red emission bands. Green emissions located at 524 nm and 552 nm corresponding to $^2H_{11/2}/^4S_{3/2} \rightarrow {}^4I_{15/2}$ transitions, respectively. Red emission band between 645 nm to 678 nm ascribed to $^4F_{9/2} \rightarrow {}^4I_{15/2}$ transition of the Er^{3+} ion. It can be found that the emission intensity increases monotonically from 0.5% to 1.25% Er^{3+} doping concentration, reaching its maximum value at 1.25%. And then the PL intensity decreases when the doping concentration arrives at 1.5%. Such concentration quenching is associated with the competition between the radiative and non-radiative transitions of the luminescent centers.

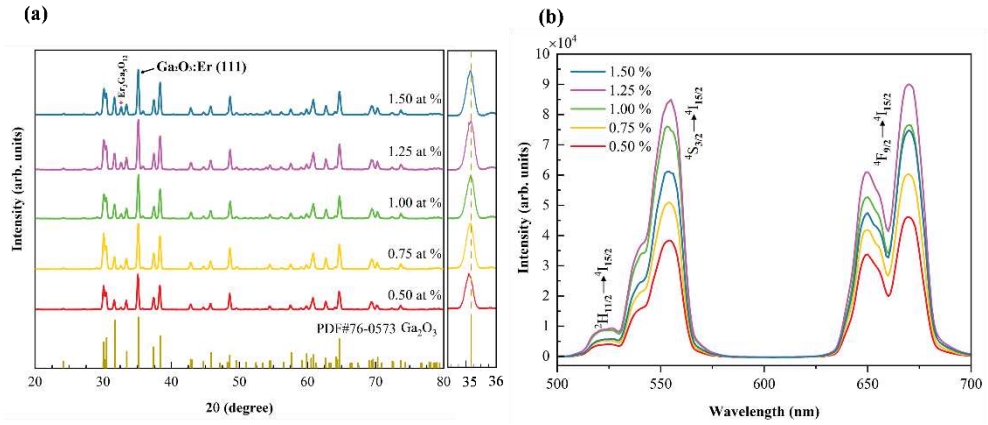

Figure 1. (**a**) XRD θ-2θ scan of Er^{3+}-doped Ga_2O_3 targets with different concentrations. Dashed lines represent the positions of the characteristic bulk Ga_2O_3: Er (111) reflections. (**b**) PL spectra of the Ga_2O_3: Er targets with different Er doping concentrations at room temperature.

Taking both structural and luminescent factors into account, Ga_2O_3:1%Er target was chosen for growing Ga_2O_3: Er thin films as well as for investigating the effect of amorphous-to-crystalline transition on the luminescent properties. It is well known that the growth temperature has a great influence on the crystallinity of Ga_2O_3 during the PLD growth. Figure 2a shows the XRD patterns of the PLD-grown Ga_2O_3: Er thin films on (0001) sapphire substrate at RT, 300 ºC, 400 ºC, and 500 ºC. The diffraction peaks at 20.4°, 41.7°, and 64.5° correspond to the (0003), (0006), and (0009) planes of sapphire, respectively. Besides the diffraction peaks of the sapphire substrate, no diffraction peaks corresponding to β-Ga_2O_3 can be found in the XRD patterns of Ga_2O_3: Er thin films grown at substrate temperatures of RT, 300 ºC, and 400 ºC. Thus, the low temperature grown Ga_2O_3: Er films tend to be an amorphous phase. As the temperature increases, three diffraction peaks located at 30.1°, 38.2° and 58.9° corresponding to β-Ga_2O_3 (400), ($\bar{4}02$) and ($\bar{6}03$) were observed at a substrate temperature of 500 ºC, indicating the formation of a crystalline β-Ga_2O_3 phase. Figure 2b illustrates the cross-sectional SEM image of the Ga_2O_3: Er thin film grown at 500 ºC. The Ga_2O_3: Er thin film grown at high temperature exhibits a smooth and flat surface, with a uniform thickness of 480 nm. Figure 2c,d show

 doi:10.20944/preprints202402.0252.v1

the surface morphology images of the Ga_2O_3: Er thin films grown at RT and 500 ºC. The RT-grown Ga_2O_3: Er thin film exhibits amorphous or poorly crystallized. And the Ga_2O_3: Er thin films grown at 500 ºC turns into crystalline phase.

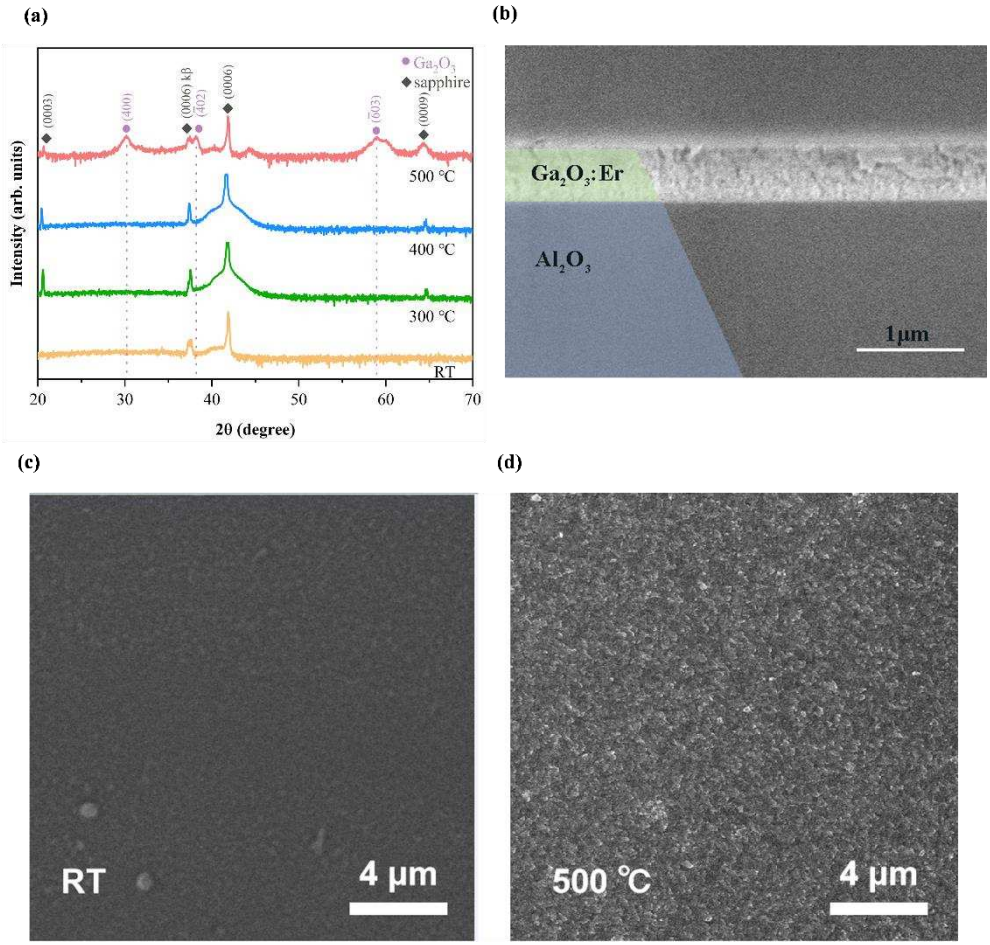

Figure 2. (**a**) XRD θ-2θ scan of Ga_2O_3: Er thin films grown at different temperatures. (**b**) The cross-sectional SEM image of the Ga_2O_3: Er thin film grown at 500 ºC. (**c**) The surface SEM image of the Ga_2O_3: Er thin film grown at RT. (**d**) The surface SEM image of the Ga_2O_3: Er thin film grown at 500 ºC.

Figure 3a shows the normalized ultraviolet-visible (UV-Vis) transmittance spectra of Ga_2O_3: Er thin films. All Ga_2O_3: Er thin films exhibit a sharp intrinsic transmittance edge at the wavelength of around 280 nm. The broad absorption band before 300 nm corresponds to the valence-to-conduction band transition of Ga_2O_3. There also exist some absorption bands centered at about 460 nm, 532 nm, and 660 nm derived from Figure 3a, which can be ascribed to the 4f-4f transition of Er^{3+} ions as well as the defects absorption. The bandgap *Eg* can be calculated by extrapolating the linear region of the plot $(\alpha hv)^2$ versus hv, as shown in Figure 3b, where h is Planck's constant, α is the linear absorption coefficient and v is the transition frequency of incident photon. It can be found that *Eg* increases from 4.10 eV to 4.22 eV for Ga_2O_3: Er thin films grown from RT to 500 ºC, respectively. As the growth temperature increases, the *Eg* gradually increases, though it remains smaller than that of pristine Ga_2O_3. One possible reason to this reduction of *Eg* due to the formation of oxygen vacancies under low-temperature growth. Moreover, Er^{3+} doping may have contributed to the reduction of the Ga_2O_3 *Eg*.

 doi:10.20944/preprints202402.0252.v1

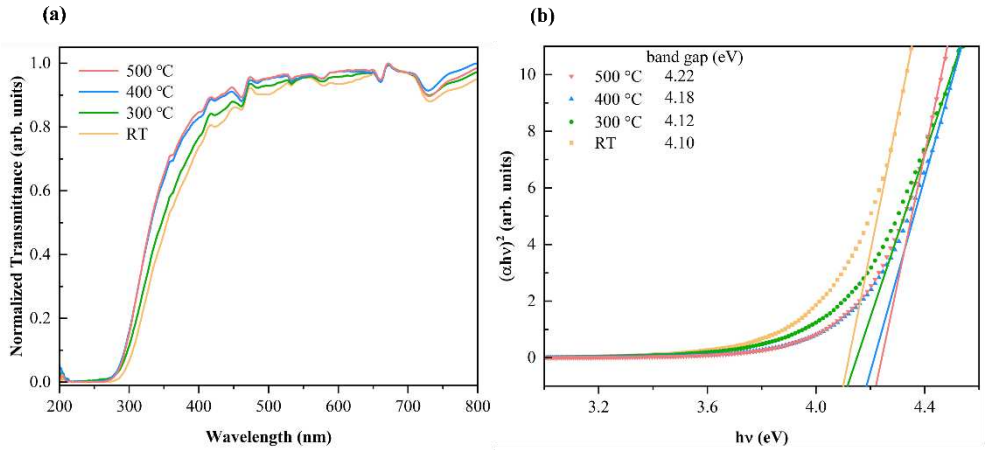

Figure 3. (**a**) Transmittance spectra of Ga_2O_3: Er thin films grown at different substrate temperatures. (**b**) The square of optical coefficient versus photon energy of Ga_2O_3: Er thin films, revealing the bandgap of different samples.

Figure 4a shows the upconversion PL spectra from Ga_2O_3: Er thin films grown under different temperatures (RT, 300 ºC, 400 ºC, and 500 ºC). The PL spectra of the Ga_2O_3: Er films were investigated under 980 nm laser diode excitation. It was found that the RT-grown Ga_2O_3: Er thin film showed almost no PL emission, suggesting that amorphous environment hinders dopant Er^{3+} ions from emitting light within an amorphous host. In other upconversion spectra, similar to the spectra of Ga_2O_3: Er targets, green emissions located at 525 nm and 549 nm arise from $^2H_{11/2}/^4S_{3/2} \rightarrow {}^4I_{15/2}$ transitions of Er^{3+} ions. While, the red emission around 659 nm corresponds to $^4F_{9/2} \rightarrow {}^4I_{15/2}$ transition of Er^{3+} ions. As seen from Figure 4a, the emission intensities increase sharply with growing temperature. Notably, the emission intensity of the Ga_2O_3: Er film grown at 500 ºC was significantly enhanced compared to that of the Ga_2O_3: Er film grown at 300 ºC, at a ratio of 127 times. This means that growth at higher temperature improves the crystallinity which in turn enhances the upconversion emission. Since the 4f-4f transitions of free lanthanide ions are Laporte forbidden, the incorporation of uneven components of the crystal field when doping into a crystalline lattice allows for intra-configurational transitions to occur [29]. Thus, compared with amorphous Ga_2O_3 host, the high-temperature grown crystalline Ga_2O_3: Er film exerts larger crystal field around the doped Er^{3+} ions, contributing to the observed enhanced upconversion emissions [30].

For further exploring the upconversion processes in Ga_2O_3: Er thin films, the pump power dependence of the upconversion emissions were investigated, as shown in Figure 4b. The number of photons can be calculated from the relationship between upconversion (UC) emission intensity (I) and incident pump power (P). Using the formula of $I \propto P^n$, where n is the number of near-infrared photons. We give the double logarithmic plot of emission intensity variation for three peaks (525 nm, 549 nm, and 659 nm) with excitation power from 0.4 to 1.8 W, which are recorded based Ga_2O_3: Er film grown at 500 ºC. Within the power range, the slope values of green and red bands can be obtained as 2.39 (525 nm), 2.31 (549 nm), 2.32 (659 nm) by a linear fit, respectively (Figure 4c). This indicates that all these upconversion emissions belong to three-photon processes in Er^{3+} ions under 980 nm excitation. Figure 4d illustrates the possible up-conversion processes through the energy level diagram of Er^{3+} ions. Upon 980 nm excitation, Er^{3+} ion can populate into $^4F_{7/2}$ energy level via the excited state absorption or energy transfer processes. Subsequently, the Er^{3+} ions relax nonradiatively to the $^2H_{11/2}$ and $^4S_{3/2}$ energy levels by the multiphoton relaxation, contributing to the green emissions at 525 nm, 549 nm, respectively. Some electrons of excited Er^{3+} ions can further relax to the $^4F_{9/2}$ level, which gives rise to the red emissions at 659 nm.

 doi:10.20944/preprints202402.0252.v1

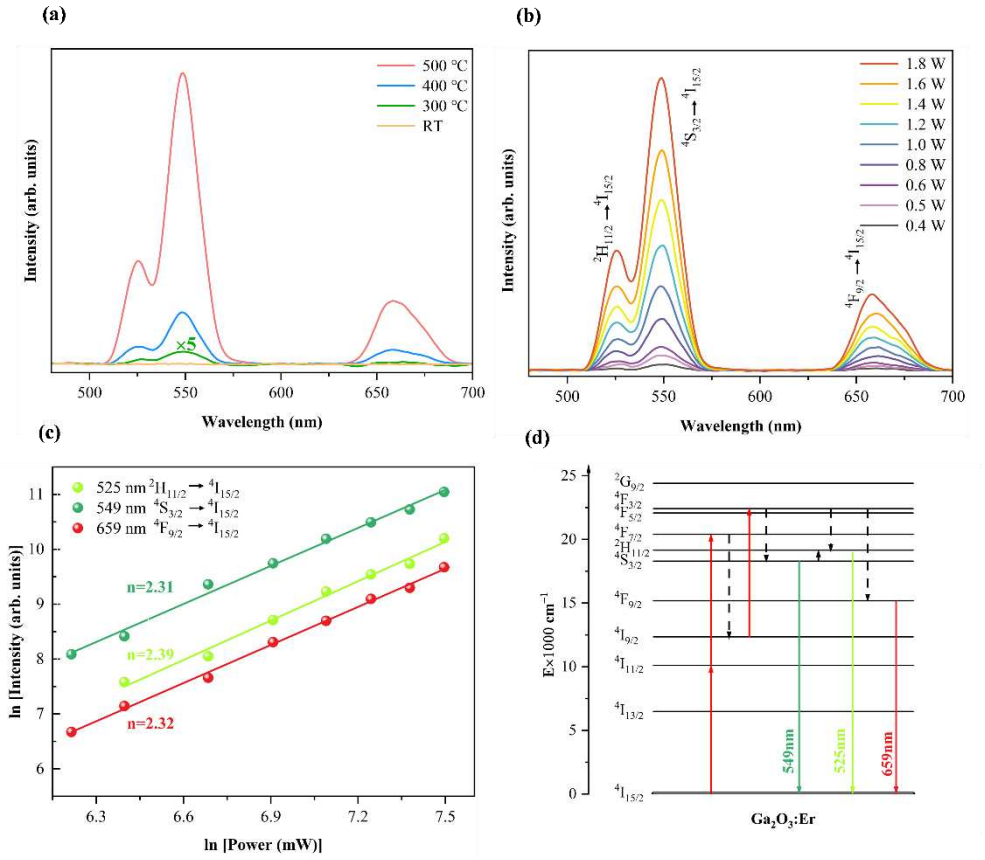

Figure 4. (**a**) The upconversion PL spectra of Ga_2O_3: Er thin films at different grown temperatures. (**b**) The upconversion emission spectra of the Ga_2O_3: Er thin film grown at 500 ºC under 980 nm laser excitation with different power densities. (**c**) Double logarithmic plot of upconversion emission intensity at 525 nm, 549 nm and 659 nm, respectively. (**d**) The Energy scheme of Er^{3+} ions and the mechanism to produce the upconversion spectra.

In the end, we investigated the fluorescence lifetime of Ga_2O_3: Er thin film grown at 500 ºC. Figure 5a shows that the lifetime at 549 nm of Ga_2O_3: Er target is about 173 μs, which is in the same order of reported Er^{3+}-doped oxide bulks. While, as shown in Figure 5b the lifetime of Ga_2O_3: Er thin film grown at 500 ºC has greatly reduced to ~4.3 μs. The strongly reduced fluorescence lifetime observed in Ga_2O_3: Er thin film may arise from the appearance of abundant defects in the as-grown thin film. These defects introduce nonradiative relax channels, resulting in the reduced lifetime of the Ga_2O_3: Er thin film.

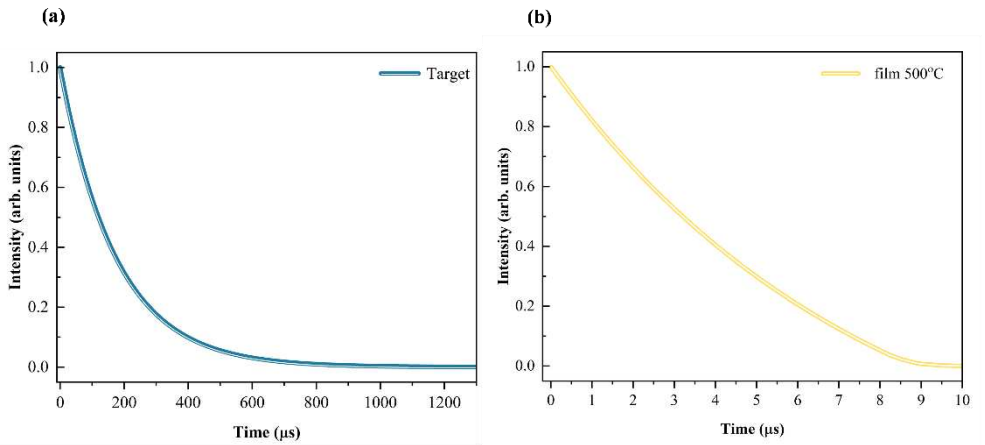

Figure 5. (**a**) PL decay curve of the Ga_2O_3: Er target with 1% concentration. (**b**) PL decay curve of the Ga_2O_3: Er thin film grown on sapphire substrate at 500 ºC.

4. Conclusions

In summary, we have investigated the amorphous-to-crystalline transition impact on the upconversion properties of lanthanide Er^{3+}-doped Ga_2O_3 thin films. Ga_2O_3: Er thin films were grown on (0001) sapphire substrate at different temperatures by PLD methods. With increasing growth temperature, Ga_2O_3: Er thin films undergo the amorphous-to-crystalline transformation, and β-Ga_2O_3 phase gradually dominates in the Ga_2O_3: Er films. There is almost no upconversion emission observed in amorphous Ga_2O_3: Er thin film. The PL intensity of the β-Ga_2O_3 phase at 500 ºC is strongly enhanced. The observed remarkable PL enhancement with increasing growth temperature is associated with the improved crystallinity of the as-grown Ga_2O_3 thin films. The appearance of abundant defects give rise to the strongly reduced lifetime in the Ga_2O_3: Er thin film. The interplay between the upconversion emission and the crystallization condition provides a feasible method to explore the intrinsic crystallinity state of Ga_2O_3. Our finding offers more insight in developing lanthanide-doped wide bandgap semiconductor Ga_2O_3 materials, which holds promise for multi-functional optoelectronic applications.

Author Contributions: Conceptualization, Y.Z., and Z.W.; methodology, H.C., J.G., X.D., T.B. and F.Z.; formal analysis, Y.L., Y.Z., D.D., J.G. and T.B.; investigation, Y.L., Y.Z., J.G., X.D. and F.Z.; data curation, Y.L. and D.D.; writing—original draft preparation, Y.L.; writing—review and editing, Y.Z. and Z.W.; supervision, Y.Z. and Z.W.; funding acquisition, Y.Z. and Z.W. All authors have read and agreed to the published version of the manuscript.

Funding: This research was funded by the National Natural Science Foundation of China (No. 12274243, 52233014, 51172208 and 12074044), the Fund of State Key Laboratory of Information Photonics and Optical Communications (IPOC2021ZT05), and the Open Fund of IPOC (BUPT, IPOC2022A02).

Data Availability Statement: The data presented in this study are available on request from the corresponding author.

Conflicts of Interest: The authors declare no conflicts of interest.

References

1. Pearton, S.J.; Yang, J.; Cary, P.H.; Ren, F.; Kim, J.; Tadjer, M.J.; Mastro, M.A. A review of Ga_2O_3 materials, processing, and devices. *Appl. Phys. Rev.* **2018**, *5*, 011301.
2. Zhang, Q.; Li, N.; Zhang, T.; Dong, D.; Yang, Y.; Wang, Y.; Dong, Z.; Shen, J.; Zhou, T.; Liang, Y.; Tang, W.; Wu, Z.; Zhang, Y.; Hao, J. Enhanced gain and detectivity of unipolar barrier solar blind avalanche photodetector via lattice and band engineering. *Nat. Commun.* **2023**, *14*, 418.
3. Hu, Z.; Cheng, Q.; Zhang, T.; Zhang, Y.; Tian, X.; Zhang, Y.; Feng, Q.; Xing, W.; Ning, J.; Zhang, C.; Zhang, J.; Hao, Y. Solar-blind photodetectors fabricated on β-Ga_2O_3 films deposited on 6° off-angled sapphire substrates. *J. Lumin.* **2023,** *255*, 119596.
4. Zhang, J.; Dong, P.; Dang, K.; Zhang, Y.; Yan, Q.; Xiang, H.; Su, J.; Liu, Z.; Si, M.; Gao, J.; Kong, M.; Zhou, H.; Hao, Y. Ultra-wide bandgap semiconductor Ga_2O_3 power diodes. *Nat. Commun.* **2022**, *13*, 3900.
5. Chen, Z.; Saito, K.; Tanaka, T.; Guo, Q. Efficient pure green emission from Er-doped Ga_2O_3 films. *CrystEngComm* **2017**, *19*, 4448-4458.
6. Luo, W.; Liu, Y.; Chen, X. Lanthanide-doped semiconductor nanocrystals: electronic structures and optical properties. *Sci. China Mater.* **2015**, *58*, 819-850.
7. Perumal, R.N.; Athikesavan, V. Structural and electrical properties of lanthanide-doped $Bi_{0.5}(Na_{0.80}K_{0.20})_{0.5}TiO_3$–$SrZrO_3$ piezoelectric ceramics for energy-storage applications. *J. Mater. Sci. Mater. Electron.* **2020**, *31*, 4092-4105.
8. Bian, T.; Zhou, T.; Zhang, Y. Preparation and Applications of Rare-Earth-Doped Ferroelectric Oxides. *Energies* **2022**, *15*, 8442.
9. Marin, R.; Jaque, D. Doping Lanthanide Ions in Colloidal Semiconductor Nanocrystals for Brighter Photoluminescence. *Chem. Rev.* **2021**, *121*, 1425-1462.
10. Xie, Y.; Song, Y.; Sun, G.; Hu, P.; Bednarkiewicz, A.; Sun, L. Lanthanide-doped heterostructured nanocomposites toward advanced optical anti-counterfeiting and information storage. *Light Sci. Appl.* **2022**, *11*, 150.

11. Dong, F.; Chen, H.; Dong, Z.; Du, X.; Chen, W.; Qi, M.; Shen, J.; Yang, Y.; Zhou, T.; Wu, Z.; Zhang, Y. Mechanically induced enhancement and modulation of upconversion photoluminescence by bending lanthanide-doped perovskite oxides. *Opt. Lett.* **2022**, *47*, 706-709.
12. Zhao, Y.; Yuan, Y.; Chen, H.; Chen, W.; Du, X.; Gong, C.; Lin, L.; Luo, W.; Liu, W.; Zhang, Y. In Situ Probing of Surface Acoustic Waves by Interfacing with Lanthanide Emitters. *Adv. Opt. Mater.* **2021**, *9*, 2001760.
13. Zhang, P.; Ke, J.; Tu, D.; Li, J.; Pei, Y.; Wang, L.; Shang, X.; Guan, T.; Lu, S.; Chen, Z.; Chen, X. Enhancing Dye-Triplet-Sensitized Upconversion Emission Through the Heavy-Atom Effect in $CsLu_2F_7$: Yb/Er Nanoprobes. *Angew. Chem. Int. Ed.* **2022**, *61*, e202112125.
14. Chen, H.; Dong, Z.; Chen, W.; Sun, L.; Du, X.; Zhao, Y.; Chen, P.; Wu, Z.; Liu, W.; Zhang, Y. Flexible and Rewritable Non-Volatile Photomemory Based on Inorganic Lanthanide-Doped Photochromic Thin Films. Adv. Opt. Mater. **2020**, *8*, 1902125.
15. Chen, H.; Dong, Z.; Zhao, Y.; Li, S.; Du, X.; Wu, Z.; Liu, W.; Zhang, Y. In-situ tailoring upconversion processes from lanthanide ions doped ferroelectric films through piezoelectric strain. *J. Lumin.* **2020**, *219*, 116914.
16. Zhang, G.; Dang, P.; Lian, H.; Xiao, H.; Cheng, Z.; Lin, J. Er^{3+}/Yb^{3+}-Based Halide Double Perovskites with Highly Efficient and Wide Ranging Antithermal Quenching Photoluminescence Behavior for Light-Emitting Diode Applications. *Laser & Photonics Rev.* **2022**, *16*, 2200078.
17. Nogales, E.; García, J.A.; Méndez, B.; Piqueras, J.; Lorenz, K.; Alves, E. Visible and infrared luminescence study of Er doped β-Ga_2O_3 and $Er_3Ga_5O_{12}$. *J. Phys. D* **2008**, *41*, 065406.
18. Khartsev, S.; Hammar, M.; Nordell, N.; Zolotarjovs, A.; Purans, J.; Hallén, A. Reverse-Bias Electroluminescence in Er-Doped β-Ga_2O_3 Schottky Barrier Diodes Manufactured by Pulsed Laser Deposition. *Phys. Status Solidi (a)* **2022**, *219*, 2100610.
19. Wu, Z.; Bai, G.; Qu, Y.; Guo, D.; Li, L.; Li, P.; Hao, J.; Tang, W. Deep ultraviolet photoconductive and near-infrared luminescence properties of Er^{3+}-doped β-Ga_2O_3 thin films. *Appl. Phys. Lett.* **2016**, *108*, 211903.
20. Deng, G.; Huang, Y.; Chen, Z.; Pan, C.; Saito, K.; Tanaka, T.; Guo, Q. Yellow emission from vertically integrated Ga_2O_3 doped with Er and Eu electroluminescent film. *J. Lumin.* **2021**, *235*, 118051.
21. Zhang, Y.; Kämpfe, T.; Bai, G.; Mietschke, M.; Yuan, F.; Zopf, M.; Abel, S.; Eng, L.M.; Hühne, R.; Fompeyrine, J.; Ding, F.; Schmidt, O.G. Upconversion photoluminescence of epitaxial Yb^{3+}/Er^{3+} codoped ferroelectric Pb(Zr,Ti)O_3 films on silicon substrates. *Thin Solid Films* **2016**, *607*, 32-35.
22. Liu, Z.; Zhi, Y.; Zhang, S.; Li, S.; Yan, Z.; Gao, A.; Zhang, S.; Guo, D.; Wang, J.; Wu, Z.; Li, P.; Tang, W. Ultrahigh-performance planar β-Ga_2O_3 solar-blind Schottky photodiode detectors. *Sci. China Technol. Sci.* **2021**, *64*, 59-64.
23. Jamwal, N.S.; Kiani, A. Gallium Oxide Nanostructures: A Review of Synthesis, Properties and Applications. *Nanomaterials* **2022**, *12*, 2061.
24. Kim, J.; Sekiya, T.; Miyokawa, N.; Watanabe, N.; Kimoto, K.; Ide, K.; Toda, Y.; Ueda, S.; Ohashi, N.; Hiramatsu, H.; Hosono, H.; Kamiya, T. Conversion of an ultra-wide bandgap amorphous oxide insulator to a semiconductor. *NPG Asia Mater.* **2017**, *9*, e359-e359.
25. Qin, Y.; Li, L.-H.; Yu, Z.; Wu, F.; Dong, D.; Guo, W.; Zhang, Z.; Yuan, J.-H.; Xue, K.-H.; Miao, X.; Long, S. Ultra-High Performance Amorphous Ga_2O_3 Photodetector Arrays for Solar-Blind Imaging. *Adv. Sci.* **2021**, *8*, 2101106.
26. Liang, H.; Cui, S.; Su, R.; Guan, P.; He, Y.; Yang, L.; Chen, L.; Zhang, Y.; Mei, Z.; Du, X.; Flexible X-ray Detectors Based on Amorphous Ga_2O_3 Thin Films. *ACS Photonics* **2019**, *6*, 351-359.
27. Hao, J.; Zhang, Y.; Wei, X. Electric-Induced Enhancement and Modulation of Upconversion Photoluminescence in Epitaxial $BaTiO_3$: Yb/Er Thin Films. *Angew. Chem. Int. Ed.* **2011**, *50*, 6876-6880.
28. Wang, Y.; Li, H.; Cao, J.; Shen, J.; Zhang, Q.; Yang, Y.; Dong, Z.; Zhou, T.; Zhang, Y.; Tang, W.; Wu, Z. Ultrahigh Gain Solar Blind Avalanche Photodetector Using an Amorphous Ga_2O_3-Based Heterojunction. *ACS Nano* **2021**, *15*, 16654-16663.
29. Fu, H.; Peng, P.; Li, R.; Liu, C.; Liu, Y.; Jiang, F.; Hong, M.; Chen, X. A general strategy for tailoring upconversion luminescence in lanthanide-doped inorganic nanocrystals through local structure engineering *Nanoscale* **2018**, *10*, 9353-9359.
30. Chen, B.; Zhang, X.; Wang, F. Expanding the Toolbox of Inorganic Mechanoluminescence Materials. *Acc. Mater. Res.* **2021**, *2*, 364-373.